Conformational dynamism for DNA interaction in *Salmonella typhimurium* RcsB response regulator

Patricia Casino, Laura Miguel-Romero, Juanjo Huesa, Pablo García, Francisco García-del Portillo and Alberto Marina.

Table of Contents:

Table S1. Primer list used in the manuscript

	Primers (5′→3′)
Wild-type cloning	FW: CAGGGACCCGGTATGAACAATATGAACGTAATTATTGCC RW: CGAGGAGAAGCCCGGTTACAGGGTGACGGAAGAGAGATAG
K180A	CCGCAGCATTgcgACCATCAGCAG TTGAGCTTCTTGGCGATTTC
Q185A	CATCAGCAGCgcgAAGAAATCGGC GTCTTAATGCTGCGGTTG
K187A	CAGCCAGAAGgcaTCGGCGATGATG CTGATGGTCTTAATGCTGC
K154A	TCTGTCGCCAgcaGAGAGCGAAG CGCTTATCGCCGTAACCG
L202D	TATCGCGCTGgacAACTATCTCTC TCATTCTCTACGCCCAGTTTC
L202F	TATCGCGCTGttcAACTATCTCTC TCATTCTCTACGCCCAGTTTC
R160A	CGAAGTATTAgccCTGTTCGCCGAG CTCTCTTTTGGCGACAGAC
R160D	CGAAGTATTAgacCTGTTCGCCGAG CTCTCTTTTGGCGACAGAC
A93D	CAACAACCCGgacATCCTGAGCG TTCATGGTCAGAACGATAATAGAC
R150A	CGGCGATAAGgctCTGTCGCCAAAAGAGAG TAACCGCCTGCGCTGATT
D56A	GTTGATCACTgccCTCTCCATGC ACATGCGCATCTAATTTCG
S58A	CACTGACCTCgccATGCCGGGAG ATCAACACATGCGCATCTAATTTCGG
H12A	TGCCGATGACgccCCGATTGTAC ATAATTACGTTCATATTGTTCATC
M88A	CGTTCTGACCgccAACAACAATCCG ATAATAGACAGGCTCGGAAAATG
E170A	CCTGGTCACCgccATCGCCAAGAAG AAGCCCTCGGCGAACAGG
S207C	CTATCTCTCTtgcGTCACCCTGA TTGAGCAGCGCGATATCATT
rcsA	FW: CCTGTTTTACTAAGGTTTATCCGAAAATA RW: TATTTTCGGATAAACCTTAGTAAAACAGG
P1$_{flhDC}$	FW: CGTCGAATTAGGAAAAATCTTAGGCA RW: TGCCTAAGATTTTTCCTAATTCGACG
KO-rcsB-Fw	GCCCAATACATGAACAATATGAACGTAATTATTGCCGATGTGTAGGCTGGAGCTGCTTC
KO-rcsB-Rv	TAAGCGTAGCGCCATCAGGCTGGGTAAACATAAAAGCGATATTCCGGGGATCCGTCGACC

Table S2. Interdomain interactions for $RcsB_{BeF}$

Subunit A Structural element	Residue	Atom type	Subunit B Structural element	Residue	Atom type	Distance
Lβα1	12(HIS)	CE1[C]	Lβα4	88(MET)	CB [C]	3.77
Lβα1	12(HIS)	CD2[C]	Lβα5	109(LYS)	C [C]	3.62
Lβα1	12(HIS)	CD2[C]	Lβα5	110(GLN)	CA [C]	3.90
α1	13(PRO)	CB [C]	Lβα5	113(PRO)	CB [C]	3.83
α1	14(ILE)	CD1[C]	α1	18(GLY)	C [C]	3.43
α1	14(ILE)	CD1[C]	α1	19(ILE)	CA [C]	3.74
α1	17(PHE)	CE2[C]	loop5	113(PRO)	CB [C]	3.78
α1	18(GLY)	C [C]	α1	14(ILE)	CD1[C]	3.55
α1	18(GLY)	CA [C]	α1	18(GLY)	CA [C]	3.49
α1	19(ILE)	CA [C]	α1	14(ILE)	CD1[C]	3.97
α1	21(LYS)	CG [C]	α1	17(PHE)	CD2[C]	3.57
Lβα4	88(MET)	SD [S]	Lβα4	88(MET)	SD [S]	3.33
Lβα4	88(MET)	CB [C]	Lβα1	12(HIS)	CE1[C]	3.78
Lβα5	109(LYS)	C [C]	Lβα1	12(HIS)	CD2[C]	3.66
Lβα5	110(GLN)	CG [C]	Lβα1	12(HIS)	CD2[C]	3.93
Lβα5	113(PRO)	CB [C]	α1	17(PHE)	CE1[C]	3.57
Lα7α8	165(GLY)	CA [C]	α10	199(ILE)	CD1[C]	3.49
Lα9α10	197(ASN)	CB [C]	Lα7α8	167(LEU)	CD1[C]	3.76
α10	199(ILE)	CD1[C]	α7	162(PHE)	CE2[C]	3.40
α10	199(ILE)	CB [C]	Lα7α8	167(LEU)	CD2[C]	3.78
α10	199(ILE)	CG1[C]	α10	198(ASP)	CB [C]	3.81
α10	200(ALA)	N [N]	Lα7α8	167(LEU)	CD2[C]	3.71
α10	202(LEU)	CB [C]	α10	202(LEU)	CD2[C]	3.82
α10	203(ASN)	ND2[N]	Lα7α8	165(GLY)	O [O]	2.90

Table S3. Structural superposition of $RcsB_{BeF}$ with other members of the NarL/FixJ subfamily

RMSD (Å) (REC- alone)	**$VraR_{BeF}$ (PDB: 4IF4)**	**$DesR_{BeF}$ (PDB: 4LDZ)**	**$Spr1814_{BeF}$ (PDB: 4ZMR)**
$RcsB_{BeF}$	1.7 (118 residues)	1.8 (118 residues)	1.7 (115 residues)
RMSD (Å) (DBD- alone)			
$RcsB_{BeF}$	1.08 (56 residues)	0.64 (43 residues)	1.67 (55 residues)
RMSD (Å) (REC-REC dimer)			
$RcsB_{BeF}$	2.5 (232 residues)	2.2 (229 residues)	2.2 (224 residues)

Table S4. Intradomain interactions for $RcsB_{BeF}$

Structural element	Subunit	Residue	Atom type	Subunit	Residue	Atom type	Distance	Structural element
α4	A	94(ILE)	CD1[C]	A	156(SER)	C [C]	3.65	α7
α3	A	68(ILE)	N [N]	A	157(GLU)	OE2[O]	3.09	α7
α4	A	94(ILE)	CD1[C]	A	160(ARG)	CB [C]	3.67	α7
Lβα3	A	58(SER)	OG [O]	A	160(ARG)	NH1[N]	3.10	α7
Lβα3	A	66(ASP)	OD1[O]	A	160(ARG)	NH2[N]	2.81	α7
Lβα3	A	62(ASP)	O [O]	A	173(ALA)	O [O]	3.41	α8
α4	A	92(PRO)	CD [C]	A	208(ALA)	C [C]	3.94	Lα10
Lβα4	A	90(ASN)	CG [C]	A	209(THR)	CG2[C]	3.23	Lα10
Lβα4	A	90(ASN)	O [O]	A	210(LEU)	N [N]	2.87	Lα10
α4	A	95(LEU)	CD1[C]	A	210(LEU)	CD1[C]	3.39	Lα10
α4	B	100(ASP)	OD2[O]	B	150(ARG)	NH2[N]	3.33	Lα6α7
α4	B	93(ALA)	CB [C]	B	195(VAL)	CG1[C]	3.61	Lα9α10
Lβα4	B	91(ASN)	ND2[N]	B	200(ALA)	O [O]	3.33	α10
α4	B	94(ILE)	CD1[C]	B	203(ASN)	C [C]	3.82	α10
α4	B	94(ILE)	CG1[C]	B	204(TYR)	CA [C]	3.82	α10
α4	B	93(ALA)	CB [C]	B	204(TYR)	CD2[C]	3.67	α10
α4	B	94(ILE)	CD1[C]	B	207(SER)	CB [C]	3.93	α10
Lβα4	B	89(ASN)	ND2[N]	B	207(SER)	OG [O]	3.37	α10
α3	B	68(ILE)	N [N]	B	207(SER)	O [O]	2.85	α10
α3	B	68(ILE)	CD1[C]	B	208(VAL)	CG1[C]	3.60	Lα10
α3	B	69(THR)	OG1[O]	B	209(THR)	OG1[O]	2.78	Lα10

Table S5. Structural superposition of $RcsB_{crossed}$ dimers.

RMSD (Å)	A-C	F-D
A-C	-	-
F-D	1.1 (410 residues)	-
G-H	1.2 (406 residues)	0.86 (408 residues)

Table S6. Structural superposition of $RcsB_{crossed}$ individual chains.

RMSD (Å)	A	C	D	F	G
C	0.8 (203 residues)	-			
D	0.8 (203 residues)	0.7 (203 residues)			
F	0.5 (206 residues)	1.0 (204 residues)	0.7 (206 residues)		
G	0.8 (203 residues)	1.0 (204 residues)	0.7 (206 residues)	0.7 (203 residues)	
H	0.8 (203 residues)	1.0 (200 residues)	0.8 (202 residues)	0.7 (202 residues)	0.7 (202 residues)

Table S7. Interdomain interactions for $RcsB_{crossed}$

Structural Element	Subunit	Residue	Atom type	Subunit	Residue	Atom type	Distance	Structural element
α8	A	170(GLU)	CD [C]	C	58(SER)	CB [C]	3.64	Lβ3α3
Lα7α8	A	166(PHE)	CE2[C]	C	58(SER)	CB [C]	3.92	Lβ3α3
α8	A	170(GLU)	OE1[O]	C	58(SER)	OG [O]	3.25	Lβ3α3
α8	A	170(GLU)	OE2[O]	C	58(SER)	OG [O]	2.70	Lβ3α3
α8	A	174(LYS)	NZ [N]	C	62(ASP)	OD1[O]	2.73	Lβ3α3
Lα7α8	A	166(PHE)	CE1[C]	C	66(ASP)	CB [C]	3.65	Lβ3α3
α7	A	160(ARG)	NH1[N]	C	66(ASP)	OD2[O]	2.57	Lβ3α3
Lα7α8	A	164(GLU)	OE2[O]	C	66(ASP)	O [O]	3.38	Lβ3α3
Lα7α8	A	164(GLU)	O [O]	C	68(ILE)	N [N]	2.93	α3
Lα7α8	A	164(GLU)	OE2[O]	C	69(THR)	N [N]	3.33	α3
Lα7α8	A	167(LEU)	CD2[C]	C	89(ASN)	CG [C]	3.77	Lβ4α4
Lα7α8	A	165(GLY)	O [O]	C	89(ASN)	ND2[N]	2.89	Lβ4α4
α10	A	202(LEU)	CD1[C]	C	91(ASN)	CG [C]	3.81	Lβ4α4
α10	A	202(LEU)	CD1[C]	C	93(ALA)	CB [C]	3.73	Lβ4α4
				C	94(ILE)	CD1[C]	3.84	Lβ4α4
Lα7α8	A	165(GLY)	CA [C]	C	94(ILE)	CD1[C]	3.77	Lβ4α4
α10	A	199(ILE)	CD1[C]	C	141(ILE)	CG2[C]	3.93	α6
α10	A	203(ASN)	OD1[O]	C	145(GLY)	O [O]	2.83	Lα6α7
Lβ3α3	A	66(ASP)	OD2[O]	C	160(ARG)	NH2[N]	3.10	α7
α3	A	69(THR)	OG1[O]	C	164(GLU)	OE2[O]	2.78	Lα7α8
α3	A	68(ILE)	N [N]	C	164(GLU)	O [O]	2.93	Lα7α8
α4	A	94(ILE)	CD1[C]	C	165(GLY)	CA [C]	3.82	Lα7α8
Lβ4α4	A	89(ASN)	ND2[N]	C	165(GLY)	O [O]	2.94	Lα7α8
α3	A	67(GLY)	CA [C]	C	166(PHE)	CE1[C]	3.99	Lα7α8
Lβ3α3	A	66(ASP)	CB [C]	C	166(PHE)	CE1[C]	3.79	Lα7α8
Lβ3α3	A	58(SER)	CA [C]	C	166(PHE)	CZ [C]	3.76	Lα7α8
Lβ3α3	A	58(SER)	OG [O]	C	170(GLU)	OE2[O]	3.20	α8
Lβ3α3	A	58(SER)	O [O]	C	173(LYS)	NZ [N]	2.96	α8
Lβ1α1	A	11(ASP)	OD2[O]	C	173(LYS)	NZ [N]	2.73	α8
Lβ3α3	A	66(ASP)	CG [C]	C	174(LYS)	CE [C]	3.84	α8
Lα9α10	A	196(GLU)	N [N]	C	194(GLY)	O [O]	2.87	Lα9α10
Lα9α10	A	194(GLY)	O [O]	C	196(GLU)	N [N]	2.94	Lα9α10
Lα9α10	A	196(GLU)	CD [C]	C	196(GLU)	CB [C]	3.77	Lα9α10
α6	A	141(ILE)	CG2[C]	C	199(ILE)	CD1[C]	3.80	α10
α4	A	91(ASN)	CG [C]	C	202(LEU)	CD1[C]	3.74	α10
α4	A	93(ALA)	CB [C]	C	202(LEU)	CD1[C]	3.79	α10
α4	A	94(ILE)	CD1[C]	C	202(LEU)	CD2[C]	3.92	α10
Lα6α7	A	145(GLY)	O [O]	C	203(ASN)	ND2[N]	2.87	α10
α10	A	204(TYR)	OH [O]	C	203(ASN)	ND2[N]	3.02	α10
α10	A	203(ASN)	OD1[O]	C	204(TYR)	OH [O]	3.03	α10
α10	A	207(ALA)	CB [C]	C	207(ALA)	CB [C]	3.69	α10

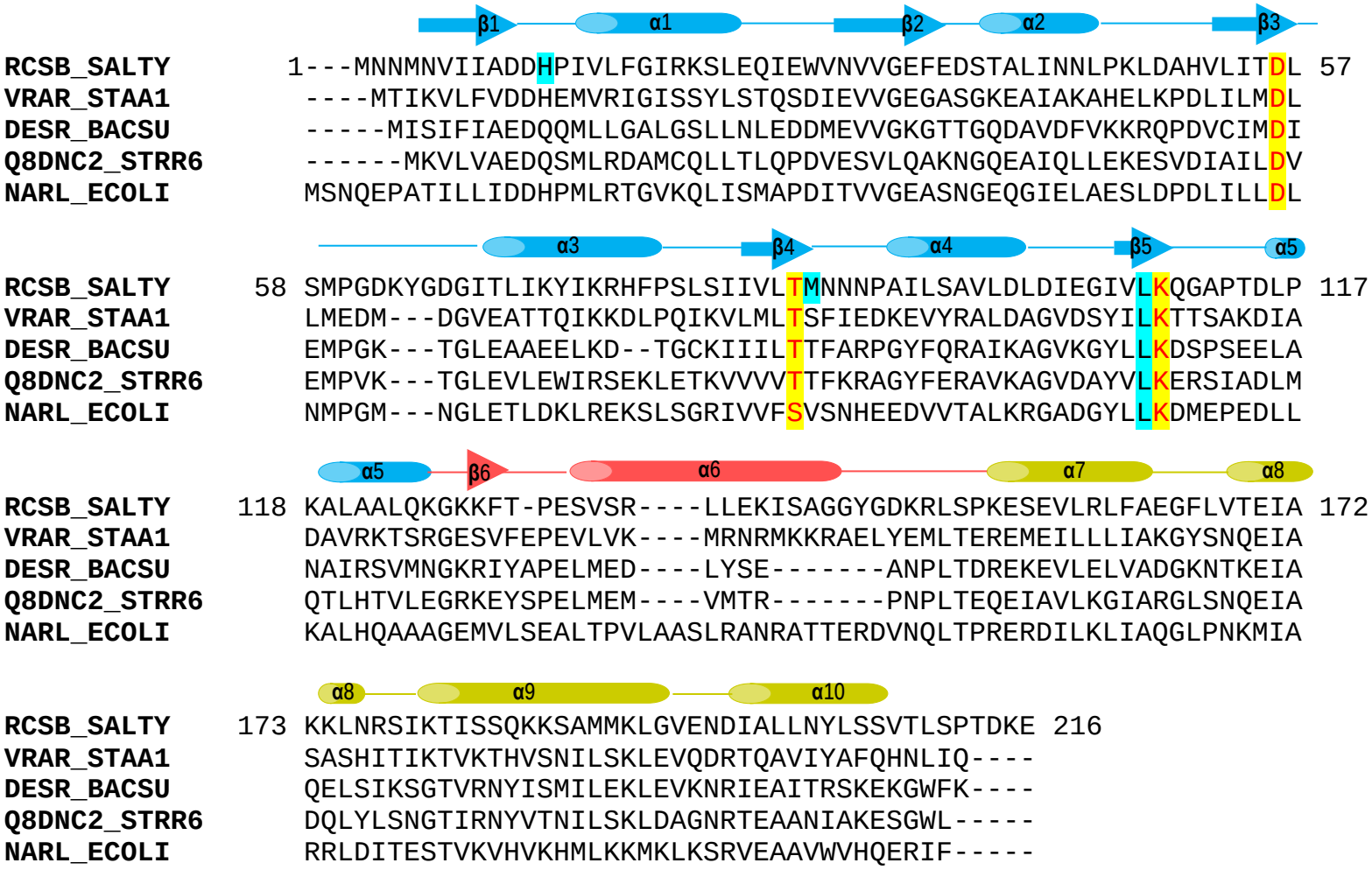

Figure S1. Protein sequence alignment of some NarL/FixJ family RRs. Sequence of the NarL family RRs RcsB from *S. typhimurium*, VraR from *S. aureus*, DesR from *B. subtilis*, NarL from *E. coli* and spr1814 from *S. pneumoniae*. The important catalytic residues, Asp/Thr/Lys, are highlighted in yellow and the conserved Leu involved in the β5-T coupling of RcsB activation in blue. The H12 involved in dimerization and M88 working as a phosphoryl gate are also shown in blue. The secondary structure of RcsB is shown in the figure labelling the structural elements of the REC domain (in blue), the REC-DBD connector (in salmon) and the DBD domain (in yellow), color coded as in Figure 1A.

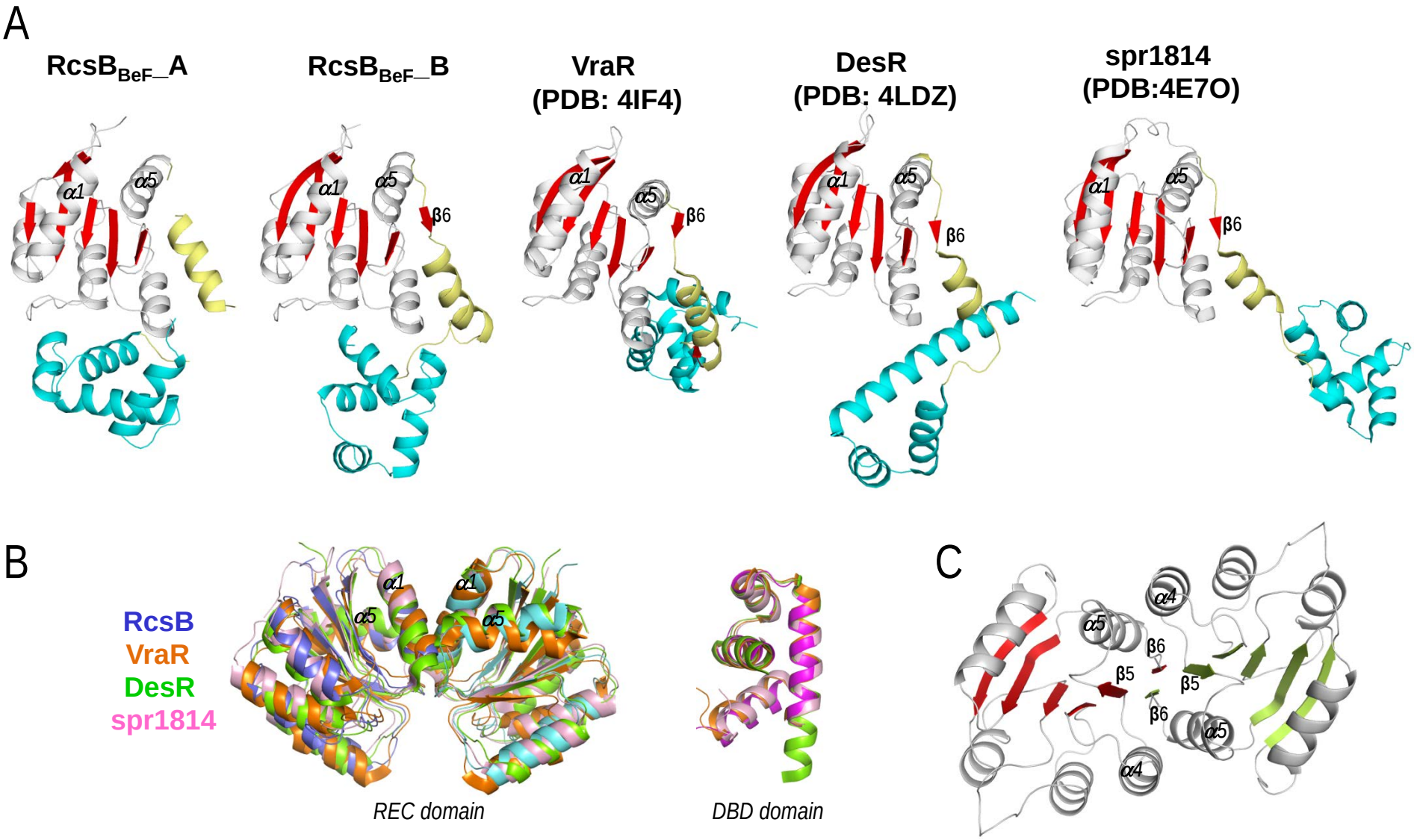

Figure S2. **Comparison of NarL/FixJ family RRs structures**. (A) Comparison of the $RcsB_{BeF}$ (monomer A and B), VraR, DesR and spr1814 monomers secondary structures highlighting the conserved β6 (in red) in the REC-DBD connector (in yellow). The DBD domain is colored in cyan and the β strands of the REC in red. (B) Superimposition of the $RcsB_{BeF}$, VraR, DesR and spr1814 phosphorylated REC dimers and the DBD domains. α1 and α5 have been labeled. (C) RcsB modeled as 4-5-5 dimer using PhoB (PDB:1ZES). β6 (in red and green) from each subunits is sandwiched between the dimerization surface introducing clashes.

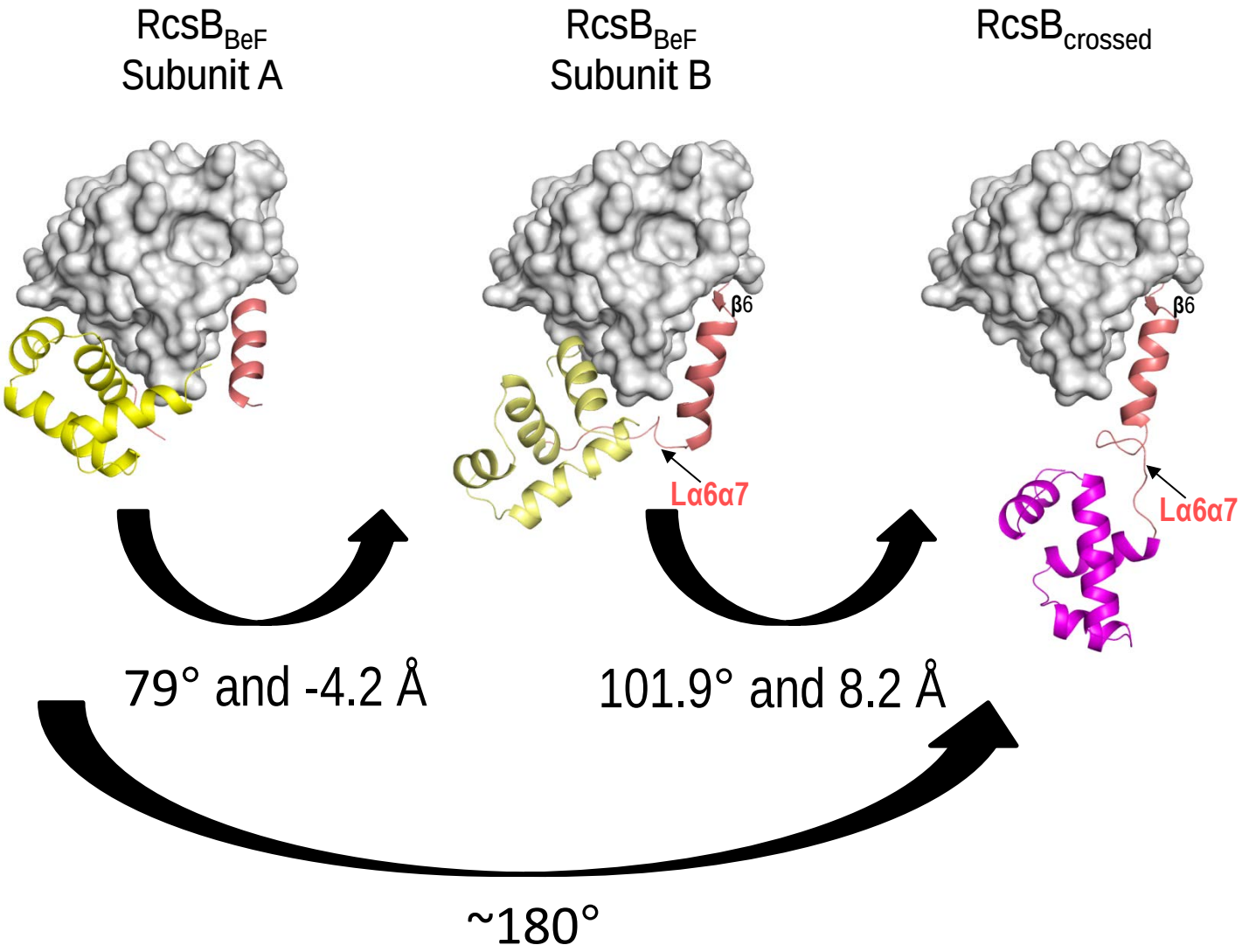

Figure S3. Interdomain dynamism in RcsB. The superposition of REC domains (in gray surface) shows that the DBD domain (in cartoon) moves 79º from its closed conformation, observed in subunit A (in cyan) to a more opened conformation observed in subunit B (in blue) of the asymmetric dimer. The DBD can relax even more and move an additional 100º to acquire the crossed conformation (in magenta). The REC-DBD connector (in yellow) in involved in the relaxation of the DBD.

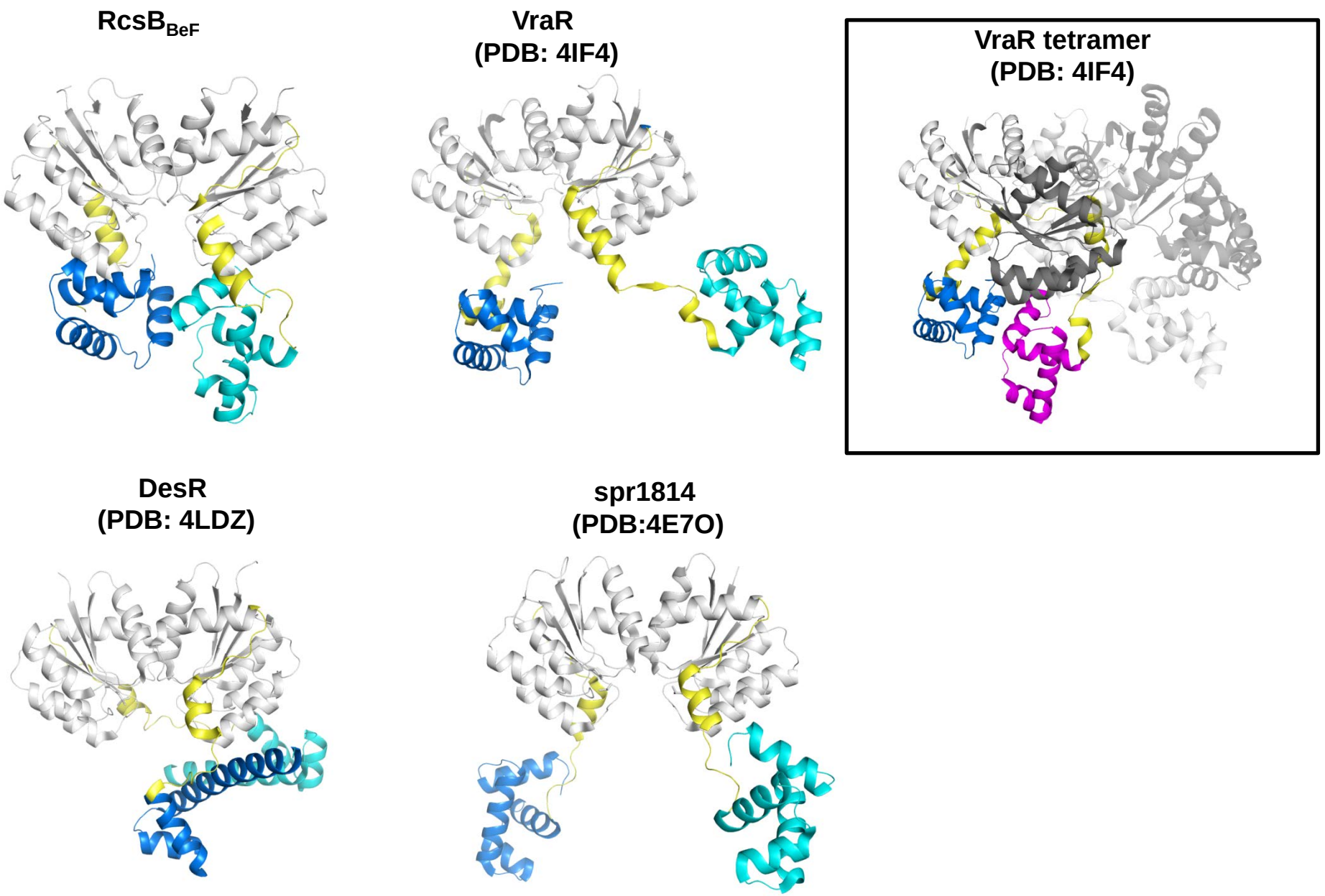

Figure. S4. Similar dimerization at the REC produces different DBD orientations in the NarL/FixJ RRs family. Dimerization α1-α5 surface in the RcsB, VraR, DesR and spr1814 NarL/FixJ RRs family. The DBD domains are in blue and the REC-DBD connector in yellow. A similar DBD dimerization as in RcsB can be obtained from the tetramer structure of VraR.

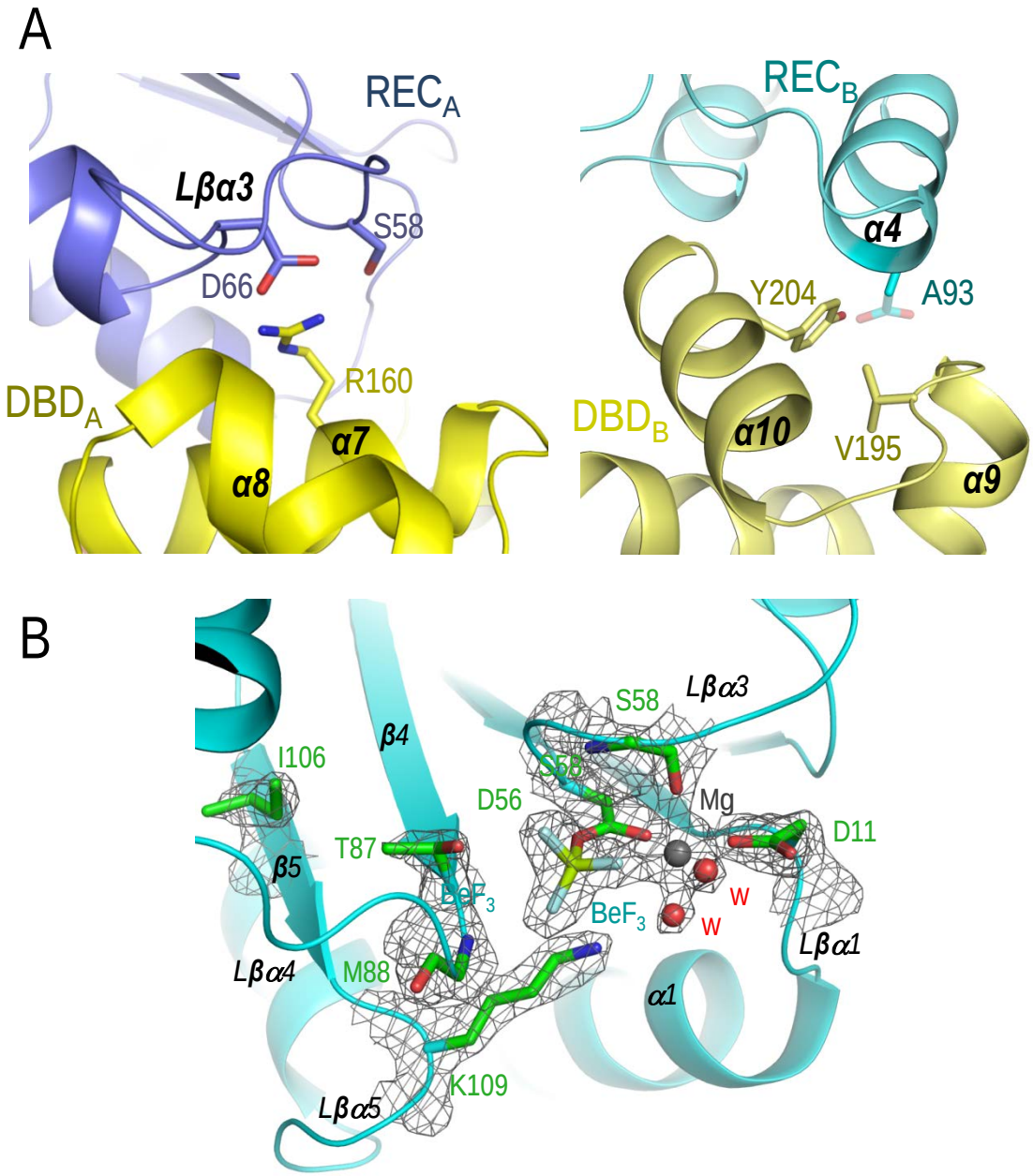

Figure. S5. (A) Asymmetry in RcsB$_{BeF}$ structure. Subunit A maintains different contacts between REC-DBD (R160 in α7 interacting with D66 in Lβ3α3) than subunit B (A93 in REC interacts with Y104 but mutation to Asp in transparency could generate clashes). (B) Electron density map (2Fo-Fc) at 2.1 Å contoured at 1σ around the catalytic residues in the active site of the RcsB$_{BeF}$ structure.

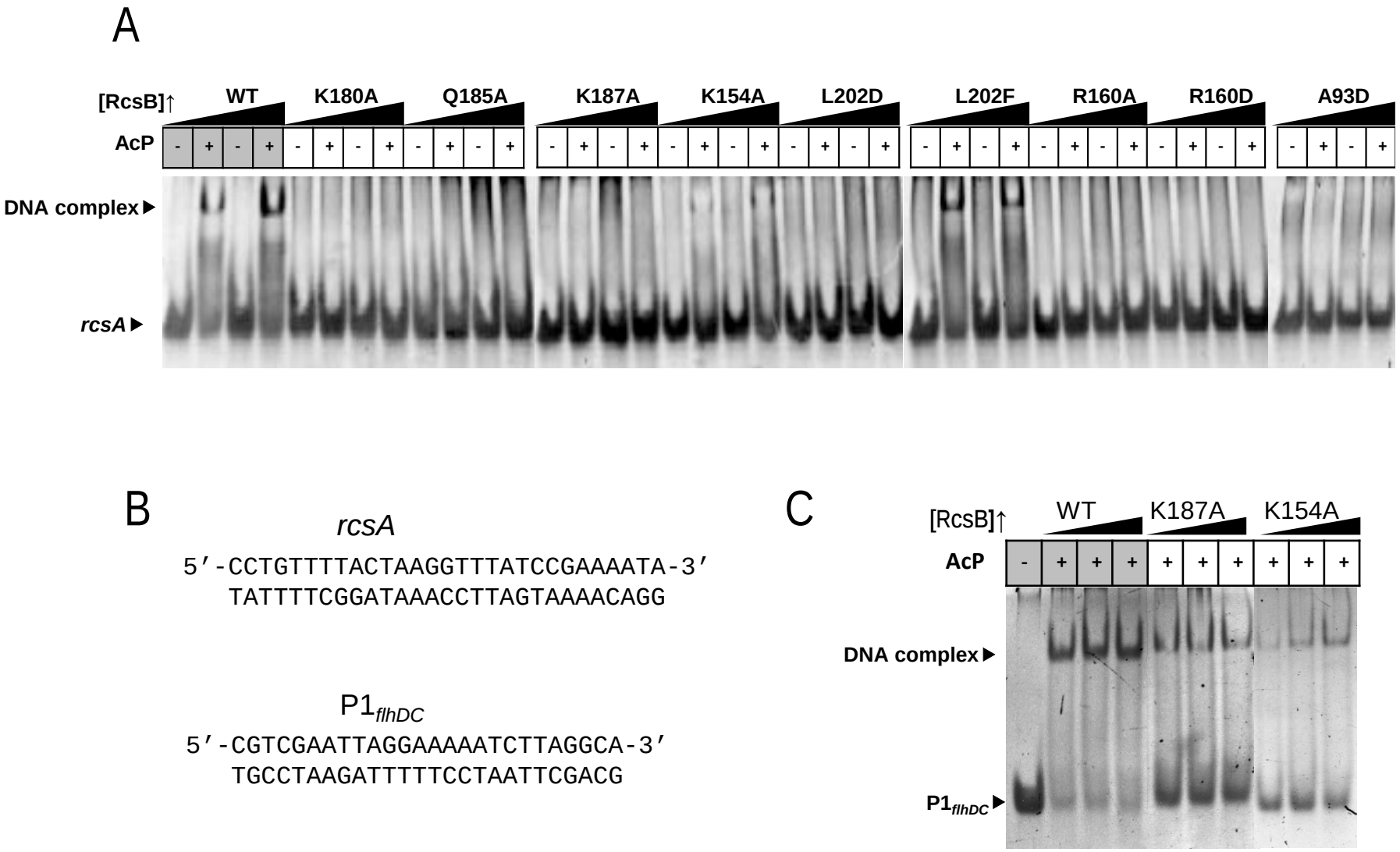

Figure S6. EMSA experiments to test binding of RcsB mutants to DNA. (A) Binding of RcsB to the *rcsA* promoter (-275 to -247) using two different concentrations of RcsB wild-type and mutants (20 and 50μM). (B) Sequence of dsDNA fragments used for EMSA experiments. (C) EMSA experiments with $P1_{flhDC}$ DNA and with wild-type, K187A and K154A mutants at 5, 10 and 20μM in presence of 50mM of AcP.

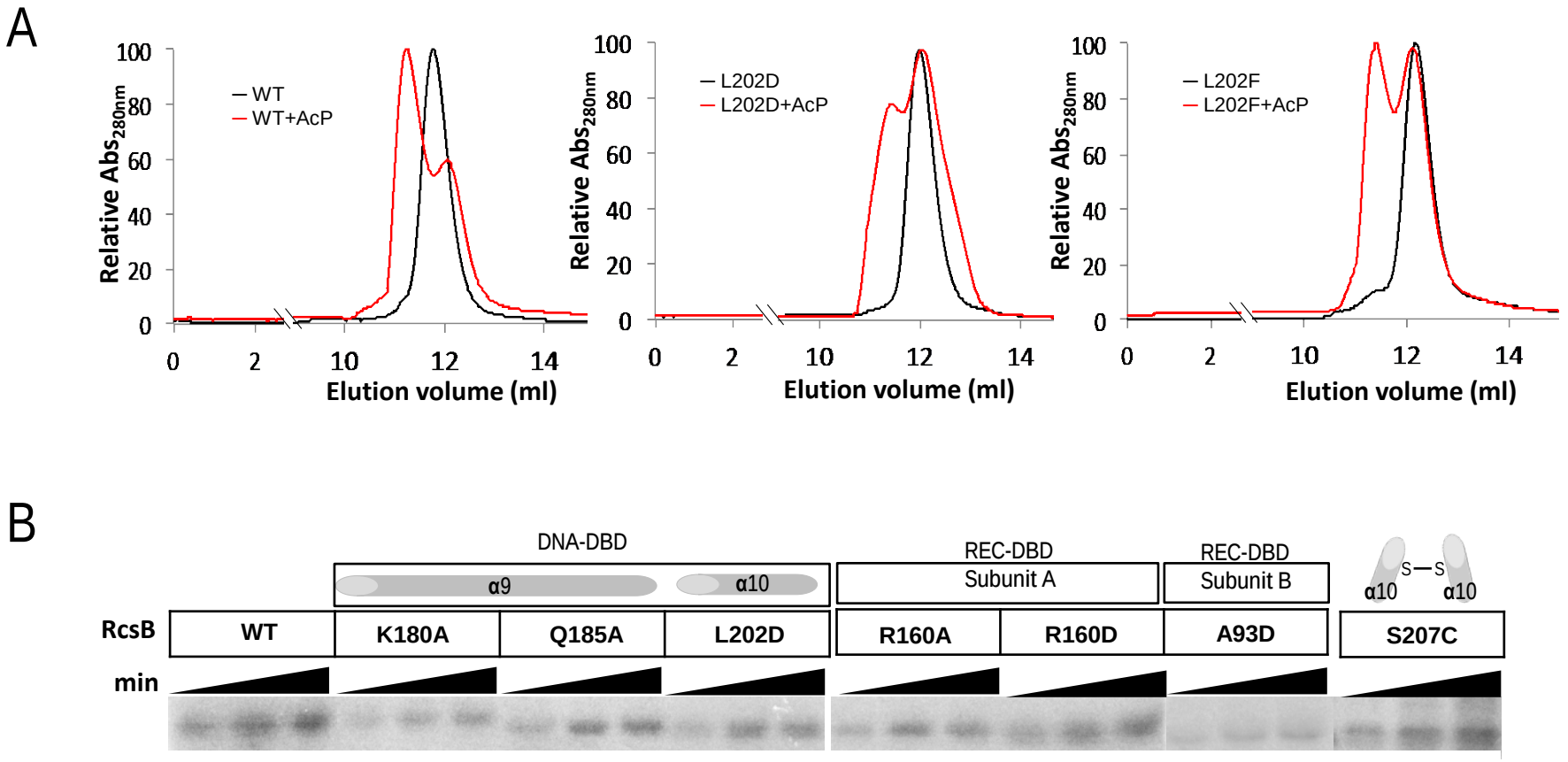

Figure S7. **Phosphorylation of RcsB mutants.** (A) Gel filtration analysis to evaluate dimer formation for mutants L202D and L202F upon phosphorylation with 50mM AcP during 30 min at 37ºC and subjected to gel filtration with Superdex 75 increase 10/300. (B) The RcsB mutants in the DNA-DBD and REC-DBD surface can be phosphorylated similarly as the wild-type incubating with [^{32}P]-acetylP for 10, 30 and 60min.

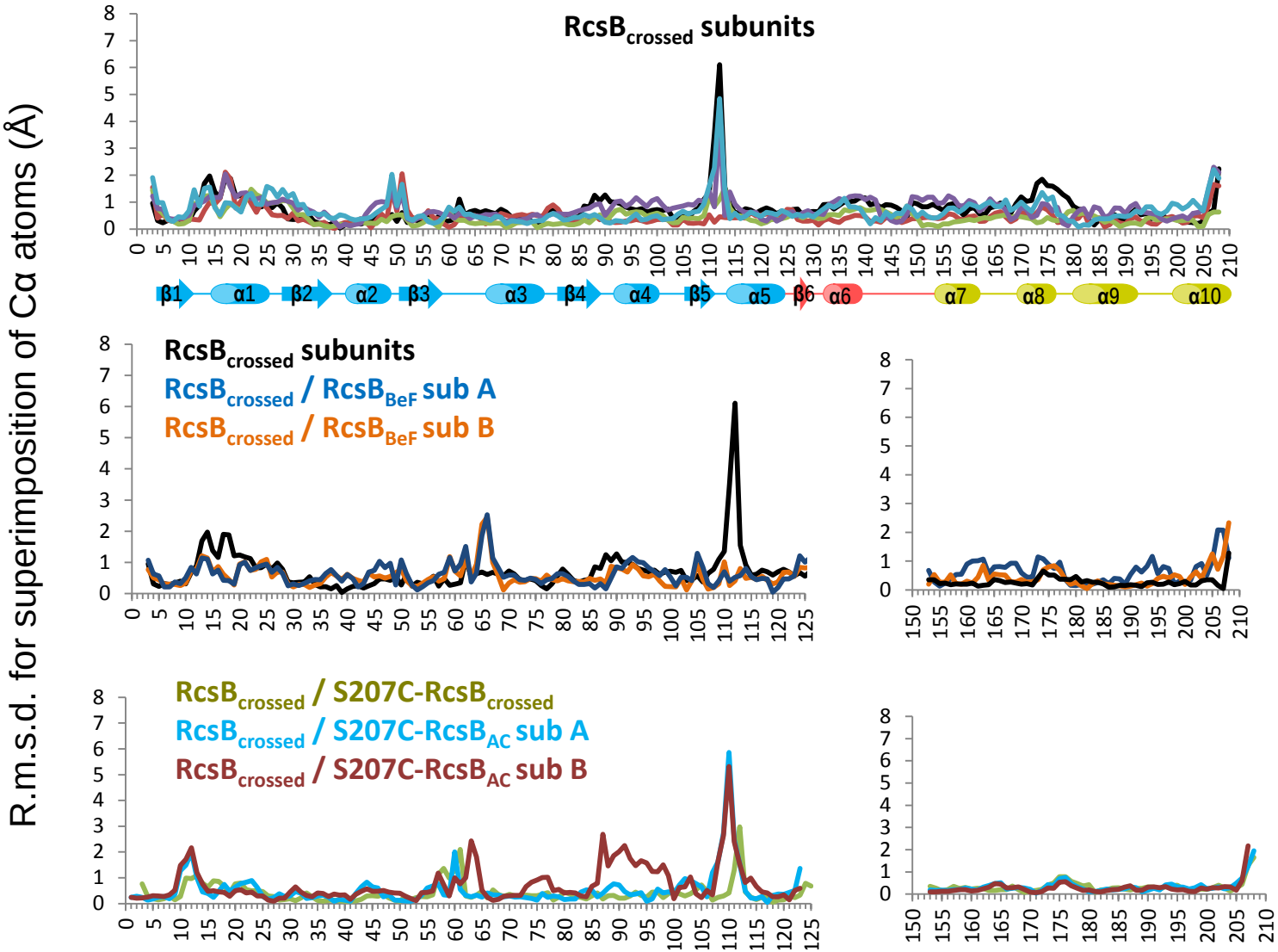

Figure S8. Superposition of RcsB wild-type and mutant structures showing residue number and secondary structure

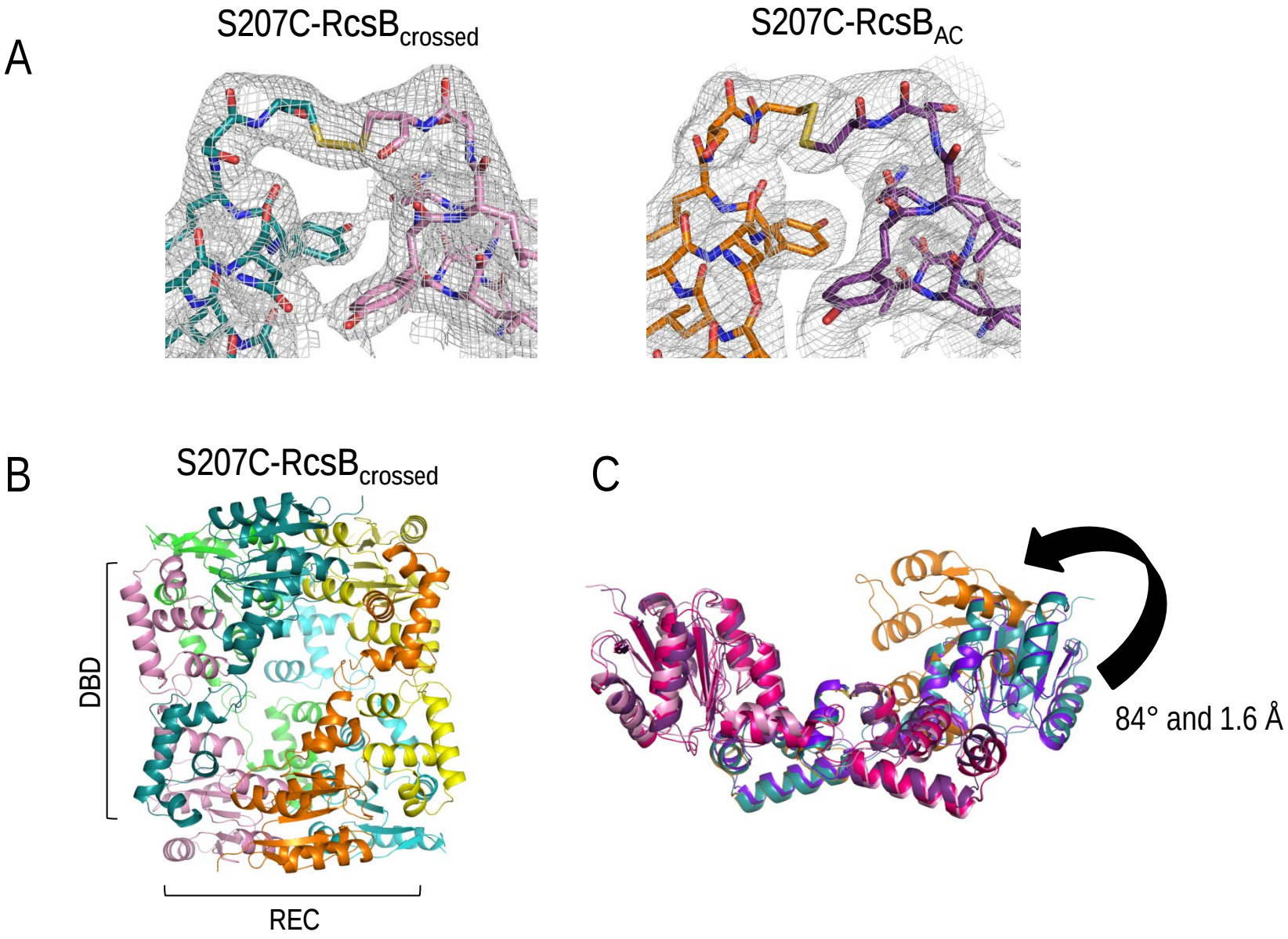

Figure S9. **Crystal structures of S207C compared to RcsB$_{crossed}$**. (A) Electron density map (2Fo-Fc) at 2.6 Å for S207C-RcsB$_{crossed}$ and 2.5 Å for S207C-RcsB$_{AC}$ contoured at 1σ around helix α10 and the disulfide bond. (B) In the crystal, S207C-RcsB$_{crossed}$ forms the hexameric structure observed for RcsB$_{crossed}$. (C) Superposition of S207C-RcsB structures with RcsB$_{crossed}$ demonstrates a similar conformation, however, the REC domain of subunit B in S207C-RcsB$_{AC}$ (in orange) has moved introducing asymmetry in the crossed conformation.

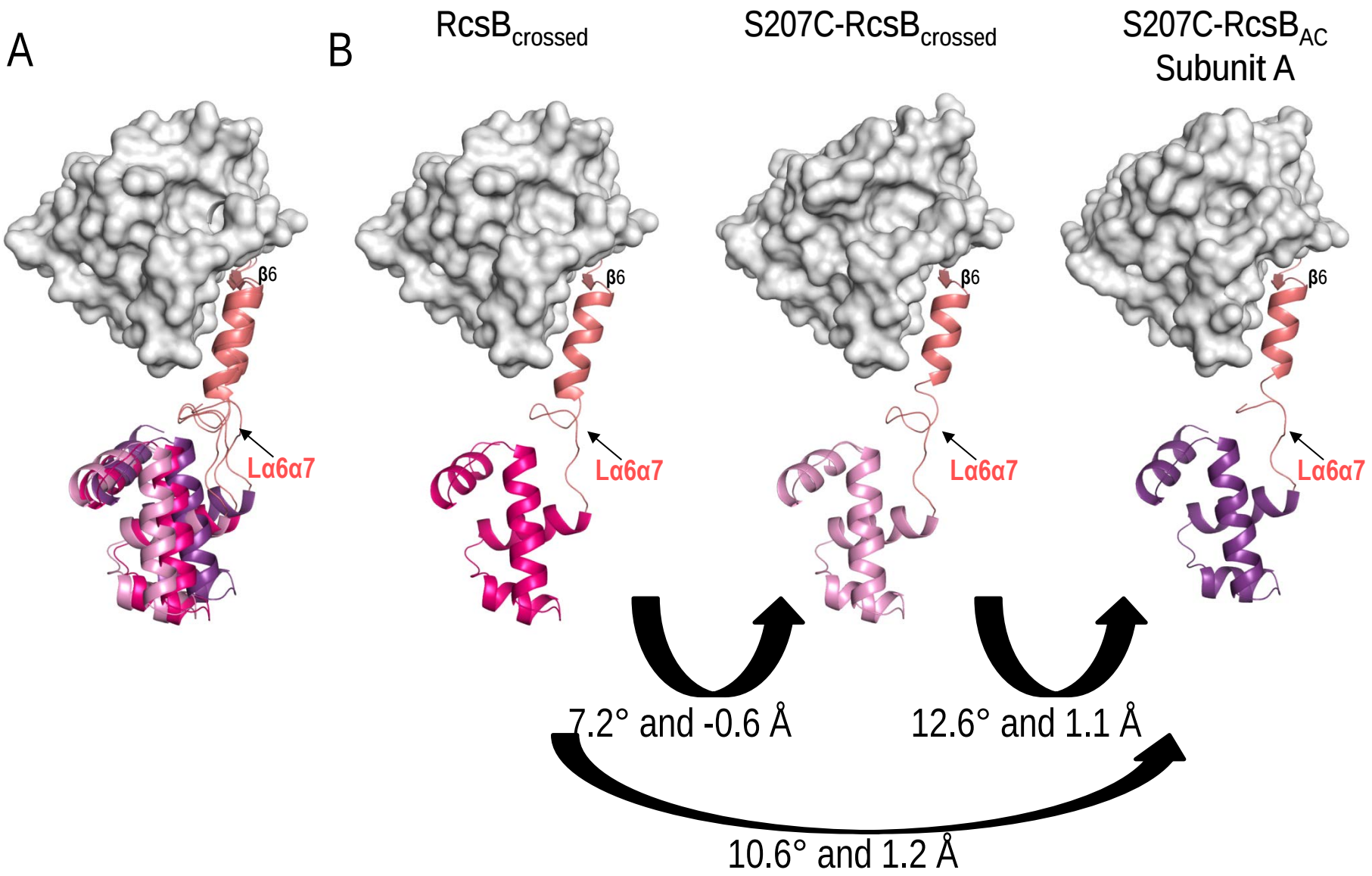

Figure S10. Similar conformation for RcsB$_{crossed}$, S207C-RcsB$_{crossed}$ and subunit A in S207C-RcsB$_{AC}$. (A) The superposition of REC domains (in gray surface) shows that DBD domain, (in darkpink for RcsB$_{crossed,}$ pink for S207C-RcsB$_{crossed}$ and violet for S207C-RcsB$_{AC}$) present a similar orientation with reduced movements. (B) The movements among the different structures fluctuated ~10°.

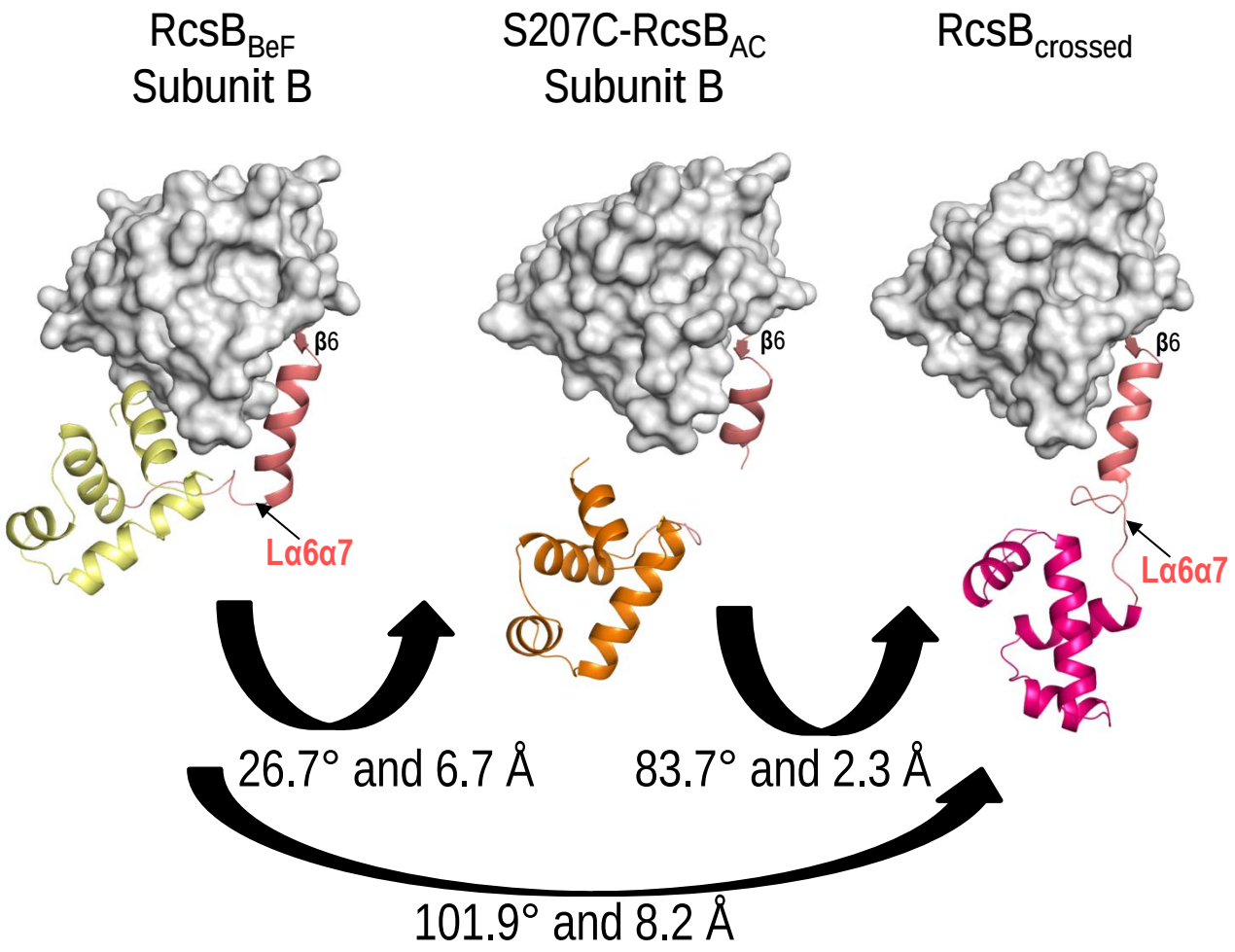

Figure S11. Dynamism of DBD domains in RcsB. Superposition of the REC domain shown in surface shows a similar orientation in all structures. The DBD domain, in cartoon, can swing from a close conformation, as observed in subunit B of $RcsB_{BeF}$ (in yellow) to a more opened conformation as observed in subunit B of S207C-$RcsB_{AC}$ (in orange) till acquires the final conformation in $RcsB_{crossed}$ reflecting the conformational dynamism of RcsB.

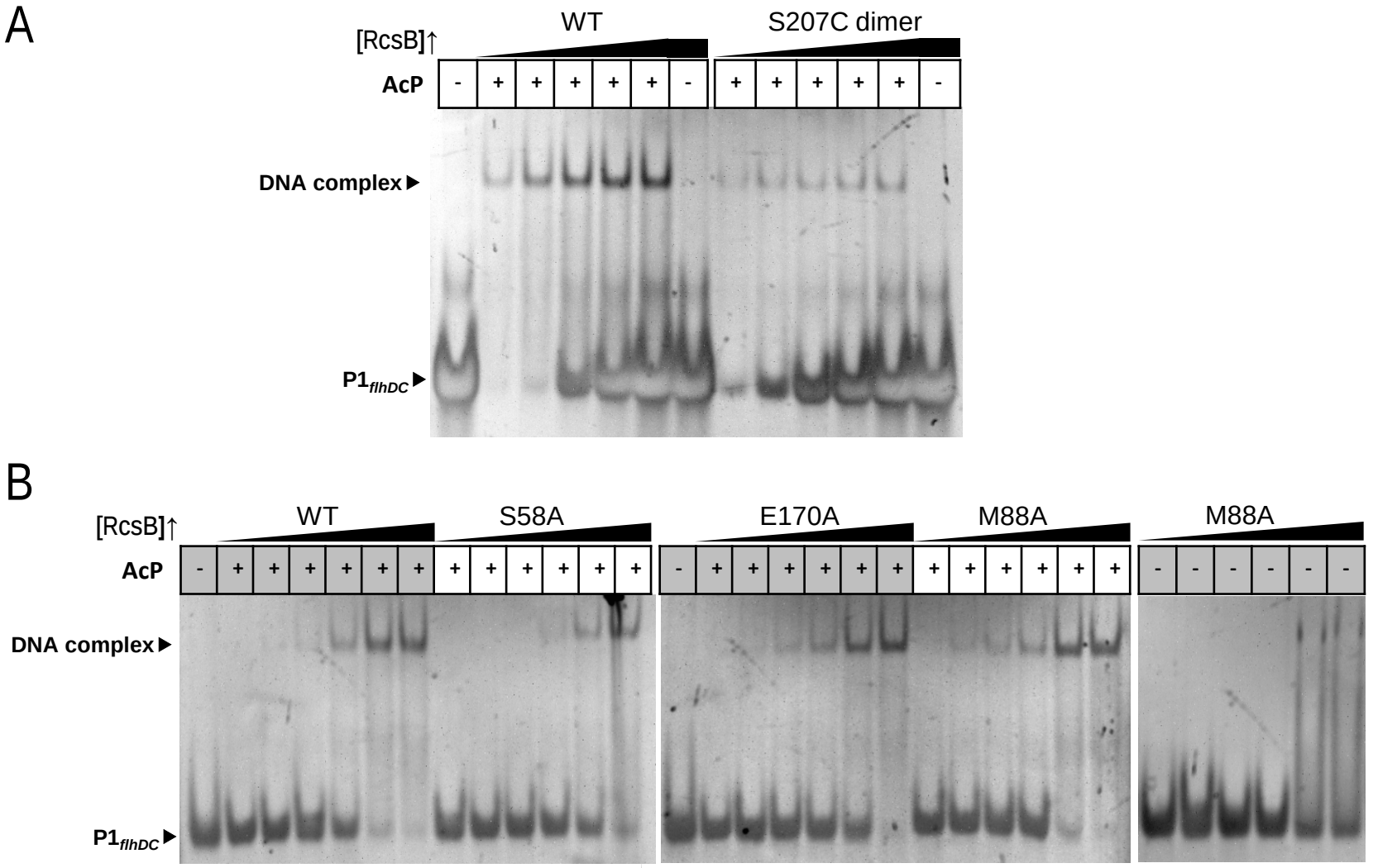

Figure S12. **EMSA experiments with RcsB mutants to test DNA-binding in a concentration dependent manner.** (A) EMSA experiment using 4 μM of wild-type and the purified dimeric specie of S207C in the presence of varying concentrations of $P1_{flhDC}$ (0.25, 0.5, 1, 2 and 4 μM) in the presence and absence of 50 mM AcP. (B) EMSA experiments using 0.5 μM of $P1_{flhDC}$ and the catalytic mutants S58A, E170A, M88A of RcsB at 0.25, 0.5, 1, 2, 4 and 6 μM in presence of 50 mM of AcP. EMSA of M88A varying protein concentration in the absence of 50 mM AcP is also shown.

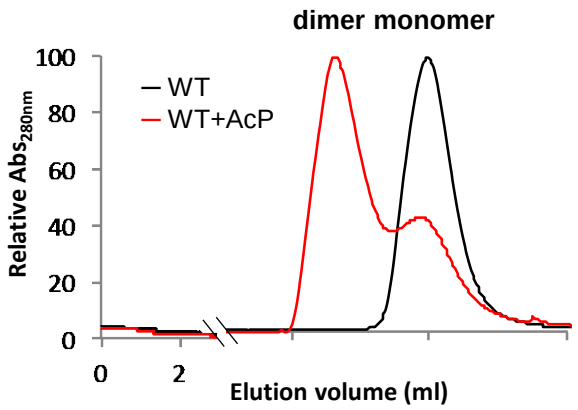

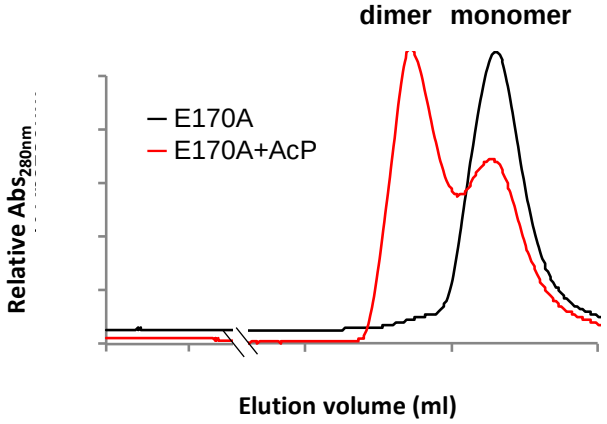

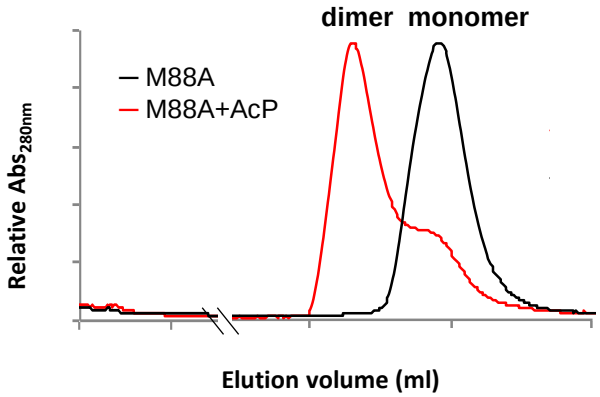

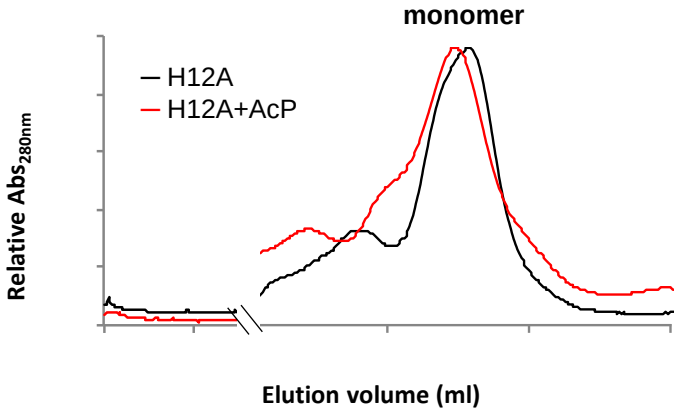

Figure S13. Gel filtration analysis to evaluate dimer formation upon phosphorylation. Wild-type RcsB and mutants M88A, E170A, H12A were phosphorylated with 50mM AcP during 30 min at 37ºC and subjected to gel filtration with Superdex 200 increase 10/300. All mutants showed dimer formation upon phosphorylation except mutant H12A. The relative proportion of dimer-monomer upon phosphorylation has been calculated and represented in a graph as bars.

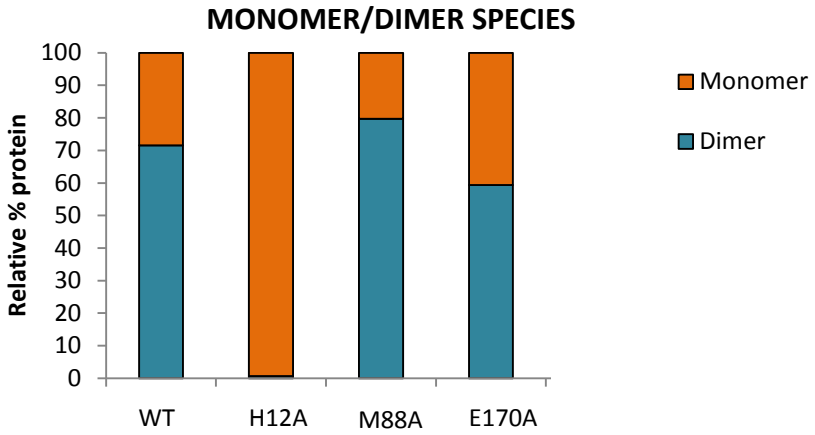

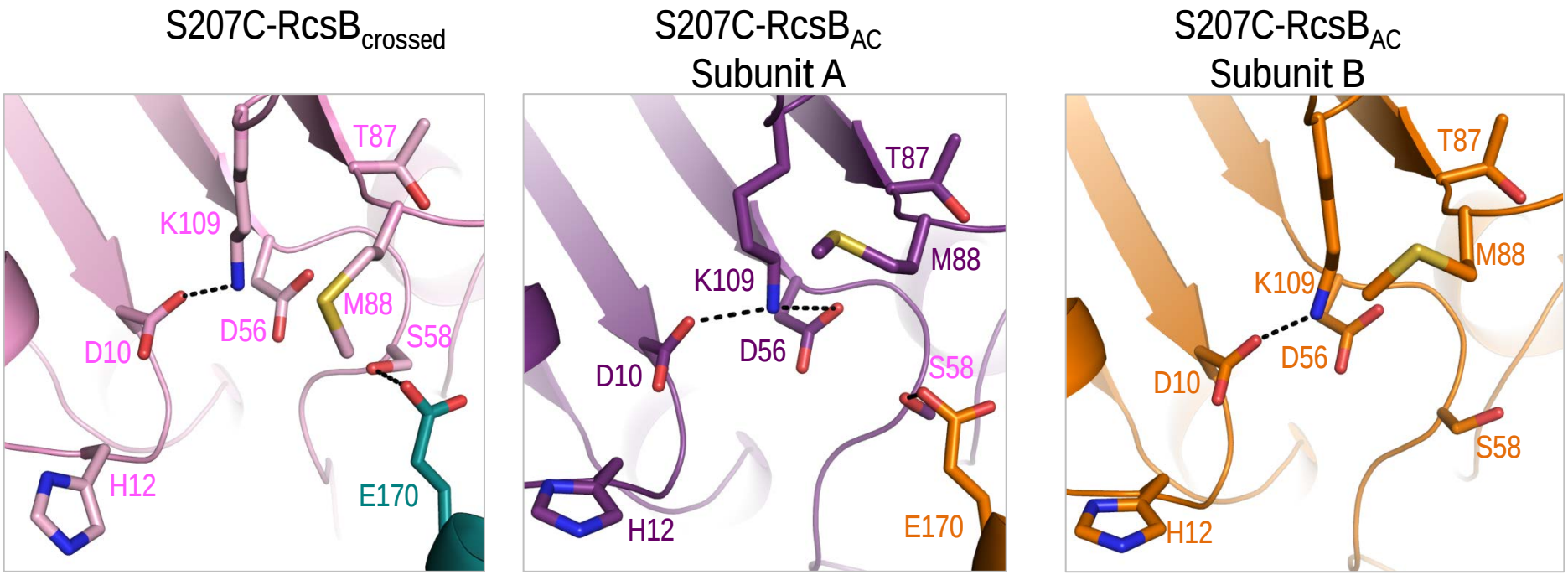

Figure S14. **Active site of S207C-RcsB structures**. Detail of the active site for S207C-RcsB$_{crossed}$ (in pink), subunit A in S207C-RcsB$_{AC}$ (in violet) and subunit B in S207C-RcsB$_{AC}$ (in orange). Catalytic residues are shown as sticks. Residue E170 coming from the DBD domain of the other subunit, in blue for S207C-RcsB$_{crossed}$ and in orange for S207C-RcsB$_{AC}$ contributes to the active site. As the REC of subunit B in S207C-RcsB$_{AC}$ has moved, E170 from the DBD of the other subunit does not longer contributes to the active site. Interactions between residues are shown as dashes lines.

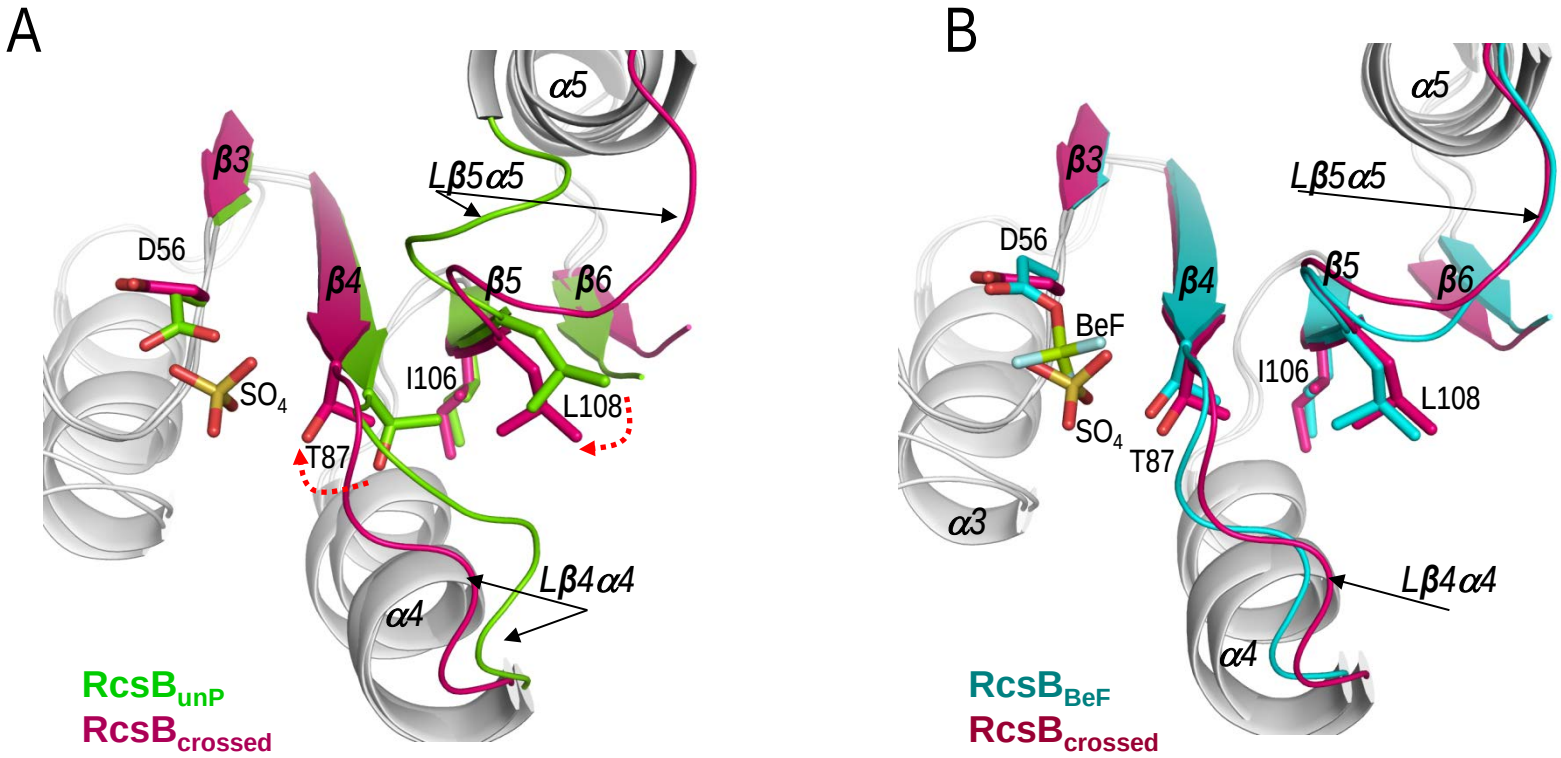

Figure S15. **Switch mechanism (β5-T coupling) of RcsB**. (A) Superimposition of the RcsB unphosphorylated ($RcsB_{unP}$; green) and phosphorylated conformation ($RcsB_{crossed}$ in darkpink) reveals movements, induced by the presence of β6, in the switch residues T87 and L108 while I106 shows the similar inward conformation. These movements produce conformational changes in Lβ4α4 and Lβ5α5. (B) Superimposition of phosphorylated $RcsB_{BeF}$ and $RcsB_{crossed}$ shows the switch residues T87 and L108 in a similar orientation, demonstrating the phosphorylated state of RcsB in both structures. Lβ4α4 and Lβ5α5 also show a similar conformation, although comparison between $RcsB_{crossed}$ subunits reveal movements in the loop Lβ5α5 which are explained by the lost of interactions at this structural element in the crossed dimer.

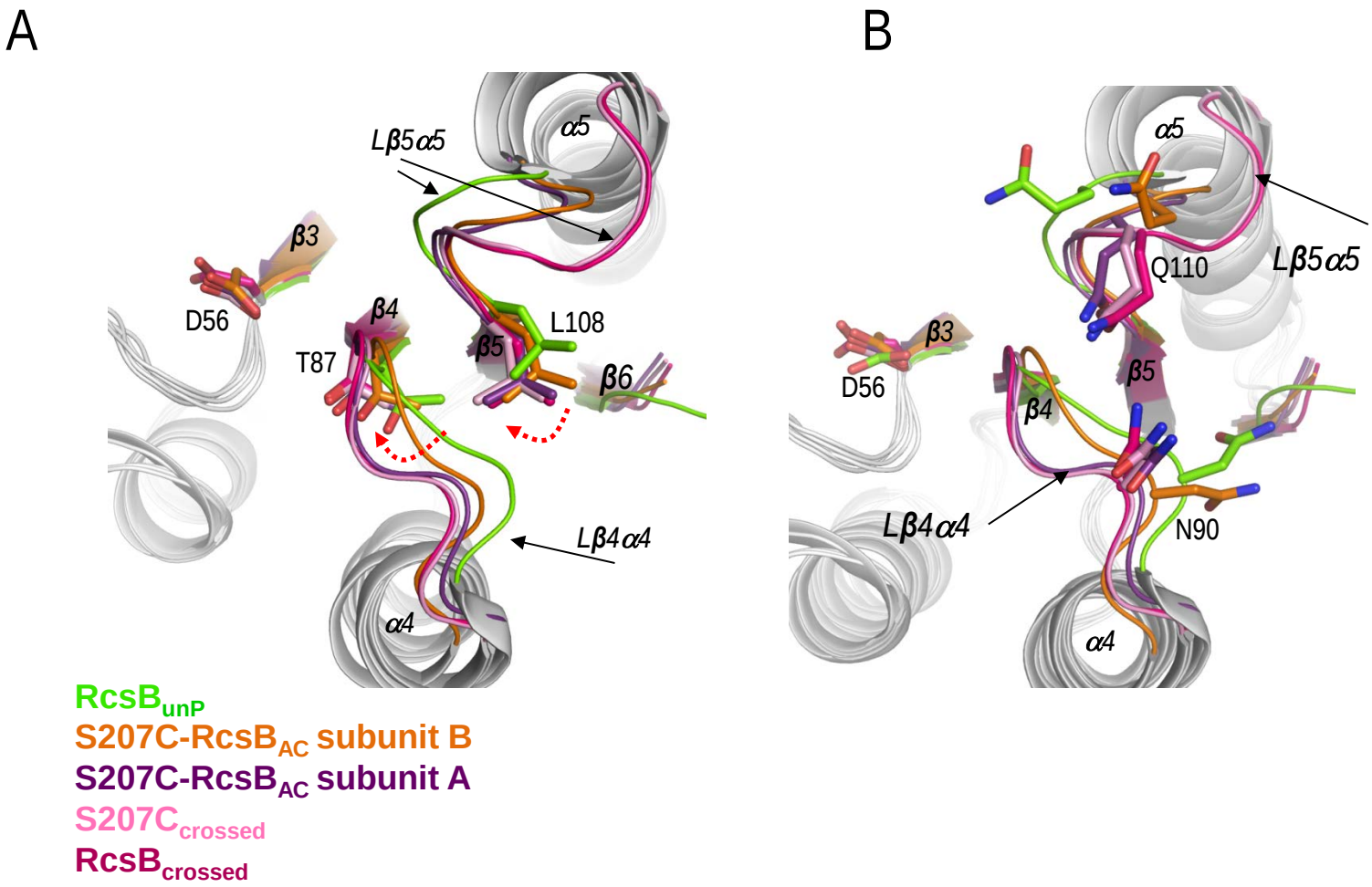

Figure S16. **Switch mechanism (β5-T coupling) of RcsB wild-type and S207C structures**. Superimposition of the RcsB unphosphorylated (RcsB$_{unP}$; green) and phosphorylated conformations (RcsB$_{crossed}$ in darkpink) with mutant S207C structures S207C-RcsB$_{crossed}$ (in pink), subunit A in S207C-RcsB$_{AC}$ (in violet) and subunit B in S207C-RcsB$_{AC}$ (in orange). (A) T87 and L108 orientations in S207C-RcsB$_{crossed}$ and subunit A in S207C-RcsB$_{AC}$ are similar to RcsB$_{crossed}$ acquiring the active form while subunit B in S207C-RcsB$_{AC}$ shows an orientation at T87 and L108 halfway inactive/active conformation. (B) Changes in orientation for T87 and L108 cause movements of Asn90 at Lβ4α4 and Gln110 at Lβ5α5 in subunit B of S207C-RcsB$_{AC}$ similar to the unphosphorylated RcsB$_{unP}$ structure in a transition state from the active to inactive conformation.